Expert Systems with Applications 39 (2012) 10600–10606

Contents lists available at SciVerse ScienceDirect

Expert Systems with Applications

journal homepage: www.elsevier.com/locate/eswa

A novel optic disc detection scheme on retinal images

Hung-Kuei Hsiao [a], Chen-Chung Liu [b], Chun-Yuan Yu [c,d], Shiau-Wei Kuo [c], Shyr-Shen Yu [c,*]

[a] Professional Development in Education, Da-Yeh University, Taiwan
[b] Department of Electronic Engineering, National Chin-Yi University of Technology, Taiwan
[c] Department of Computer Science and Engineering, National Chung-Hsing University, 250, Kuo-Kuang Rd., Taichung 402, Taiwan
[d] Department of Computer and communication Engineering, Nan Kai University of Technology, Taiwan

ARTICLE INFO

Keywords:
Optic disc
Illumination correction
GVF snake
Supervised classification
Retinal image

ABSTRACT

Robust and effective optic disc detection is a necessary processing component in automatic retinal screening systems. In this paper, optic disc localization is achieved by a novel illumination correction operation, and contour segmentation is completed by a supervised gradient vector flow snake (SGVF snake) model. Conventional GVF snake is not sufficient to segment contour due to vessel occlusion and fuzzy disc boundaries. In view of this reason, the SGVF snake is extended in each time of deformation iteration, so that the contour points can be classified and updated according to their corresponding feature information. The classification relies on the feature vector extraction and the statistical information generated from training images. This approach is evaluated by means of two publicly available databases, Digital Retinal Images for Vessel Extraction (DRIVE) database and Structured Analysis of the Retina (STARE) database, of color retinal images. The experimental results show that the overall performance is with 95% correct optic disc localization from the two databases and 91% disc boundaries are correctly segmented by the SGVF snake algorithm.

1. Introduction

Diabetic retinopathy is a chronic disease which is the primary cause of blindness in the working population of the developed world (Aquino, Gegúndez-Arias, & Marín, 2010; Manivannan, Sharp, Phillips, & Forrester, 1993; Sinthanayothin, Boyce, Cook, & Williamson, 1999; Taylor & Keeffe, 2001). Therefore, the early detection and diagnosis of diabetic retinopathy is a very important procedure from retinal images.

Optic disc detection is a very important task in retinal image analysis (Akita & Kuga, 1982; Lu & Lim, 2011). In normal retinal images, the optic disc generally appears as bright, yellowish, circular or slightly oval shape, roughly one-sixth the width of the image in diameter (Hoover & Goldbaum, 2003). Any change in the structure of the optic disc is a sign of various retinopathies especially for glaucoma (Li & Chutatape, 2004); therefore, the shape of optic disc is often used to evaluate abnormal retinal features (Ter Haar, 2005; Xu, Chutatape, Sung, Zheng, & Kuan, 2007). On the basis of the geometric relationships between the optic disc location and the vascular structure, the central macula (fovea) can be approximately located (Sinthanayothin et al., 1999; Tobin, Chaum, Govindasamy, & Karnowski, 2007).

Since the retinal blood vessels radiate from the optic nerve head, the optic nerve head is also used as a beginning point for vessels tracking (Lalonde, Gagnon, & Boucher, 2000; Sinthanayothin et al., 1999; Tolias & Panas, 1998). Furthermore, the optic disc may be identified as part of exudates regions, because the colors of the optic disc and the bright exudates are similar. It is evident that accurate optic disc identification refines the segmentation of the exudates regions (Osareh, 2004; Walter, Klein, Massin, & Erginary, 2002). The optic disc identification is fundamental for organizing a relation within retinal images, and is important to computer assisted diagnosis.

Identifying the optic disc region becomes more complicated due to the presence of retinopathy such as large exudative lesions or bright artifactual features. Sinthanayothin et al. (1999) assume that the retinal lesions have a lower variance of intensity than that of the optic disc area, in which the optic disc is approximated by identifying the largest local variation with a 80×80 window size. However, Lowell et al. (2004) had already shown that this algorithm often fails in retinal images with a large number of white lesions, light artifacts or strongly visible choroidal vessels. Besides, Walter et al. (2002) proposed another algorithm applied by shade-correction and calculated the local variation of the image for optic disc localization, in which the accurate optic disc contour

* Corresponding author. Tel.: +886 4 22840497x807; fax: +886 4 22853869.
E-mail addresses: hkhsiao@mail.dyu.edu.tw (H.-K. Hsiao), ccl@ncut.edu.tw (C.-C. Liu), t112@nkut.edu.tws (C.-Y. Yu), 9756046@cs.nchu.edu.tw, pyu@nchu.edu.tw (S.-S. Yu).

0957-4174/$ - see front matter © 2012 Elsevier Ltd. All rights reserved.
doi:10.1016/j.eswa.2012.02.157

was determined by morphological filtering techniques and watershed transformation. The resulted contour was slightly distorted due to the outgoing vessels.

A template matching algorithm was provided by Lalonde, Beaulieu, and Gagnon (2001), which is Hausdorff-based template matching in combination with pyramidal decomposition technique. Initially, a large scale object is tracked by means of multiresolution pyramidal decomposition in the green band image, and hence the presence of small bright retinal lesions such as exudates is reduced. Then the Hausdorff distance is used to measure the matching degree between the circular template and optic disc candidate regions with different scales, the region with the highest confidence value corresponds to the optic disc location. Later on, Osareh et al. (2004) proposed another template matching algorithm to locate the optic disc. In their algorithm, the template image are obtained by averaging the color-normalized optic disc region in 25 fundus images, and then the correlation coefficient is used to indicate the best match between the template and the candidate regions. Lowell et al. (2004) showed that the template matching approach is effective, but may be highly complex.

Li and Chutatape (2004) proposed a method by applying the machinery of principal component analysis (PCA) and a modified active shape model (ASM) for optic disc identification. To create a disc space, the authors manually cropped 10 sub-images from the optic disc regions for training. Each training image is described in a vector format, and the PCA transform is employed to get the first six eigenvectors representing the training set. The optic disc is identified as the region with the minimum Euclidian distance projection, which indicates the similarity of the template vectors. However, the shape model may not be suitable to detect the various disc shapes from many pathological changes.

Several algorithms based on retinal blood vessels for locating the optic disc have been investigated. However, the retinal vessels segmentation is a complicated job and the false vessel detection will greatly affect the subsequent operations. Hoover and Goldbaum (2003) proposed a fuzzy convergence scheme in order to decide the convergence point of vessels (optic disc location). Foracchia, Grisan, and Ruggeri (2004) identified the optic disc by means of fitting a parametric geometrical model to the main vessels. Akita & Kuga, 1982 tracked the parent–child relationship among the retinal vascular system for locating the optic disc.

General-purpose detection techniques usually fail to accurately identify the optic disc due to non-uniform illumination and vessel occlusion. On one hand, the appropriateness of the automatic localization depends deeply on whether the illumination is uniform or not, and on the other hand, vessel occlusion may lead to unacceptable contour segmentation. In order to correct these two technical defects, this paper presents a novel algorithm for automatic localization and segmentation of the optic disc in retinal fundus images. Optic disc localization is achieved by using a novel illumination correction operator, which results in a significant contrast between the optic disc and background. Besides, the boundary of the optic disc is extracted based on the supervised gradient vector flow snake (SGVF snake) model combined with supervised classification. The classifier is embedded into GVF snake deformation in order to detect the false contour points, and then the contour points will be updated to the correct edge position. Therefore, the proposed algorithm enables the resulted contour to be more robust for vessel interference and fuzzy disc boundaries.

The remainder of this paper is organized as follows. Section 2 describes the proposed optic disc detection methodology on a retinal image. Section 3 presents the experimental results. Finally, the conclusions of this paper are presented in Section 4.

2. Proposed methods

This paper proposes a new approach for optic disc detection, which can be divided into two phases: location and segmentation. The former focuses on locating the optic disc, and the latter estimates the optic disc contour. Fig. 1 shows a flow chart of the proposed scheme. Details of the presented optic disc scheme are described in the following subsections.

For our application, the optic disc is localized as the brightest area in the fundus image after illumination correction operator. The subsequent processes inspired by Xu et al. (2007) present the SGVF snake algorithm that combines GVF snake with supervised classification for optic disc segmentation.

2.1. Optic disc localization

The optic disc localization is essential to retinal image analysis. It is evident that accurate optic disc identification refines the segmentation of the exudates regions. The localization phase proposed in this paper combines the illumination correction processing stage and the estimating stage of optic disc location. The illumination correction operator works on the green band image, because the green band exhibits the best contrast in the retinal image.

2.1.1. Illumination correction

The illumination in retinal images is non-uniform due to an optical aberration, which is the result of an improper focusing of light through an optical system (Hoover & Goldbaum, 2003). Youssif, Ghalwash, and Ghoneim (2007) showed that the non-uniform illumination through the image greatly affects the accuracy of optic disc localization. In order to remove uneven background intensity, the illumination correction operator with the following equation is proposed:

$$I'(x,y) = I(x,y) - \frac{\mu_N(x,y)}{0.1 + \sigma_N(x,y)} \tag{1}$$

where $\mu_N(x,y)$ and $\sigma_N(x,y)$ are the mean and standard deviation of the pixel values within an $N \times N$ window, respectively. Since the region of interest (ROI) of the retinal image is roughly circular and the $N \times N$ window is square, the pixel number applied when the window is in the interior is more than the pixel number applied near the border of the ROI. Thus, when applying the operator to border pixels, the out-of-the ROI pixel values in the $N \times N$ window are replaced by the mean pixel value of the remaining pixels in the window. As stated in Sinthanayothin et al. (1999), yellowish optic disc appears as bright patterns in retinal images, and the grey level variation is high due to the outgoing vessels. The illumination correction operator preserves bright regions associated with the optic disc which has large local variation, and generates a significant contrast between the optic disc and background (Fig. 2(b)).

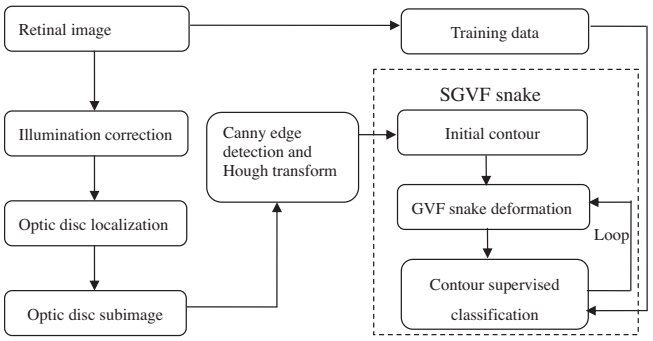

Fig. 1. Flow chart of optic disc detection process.

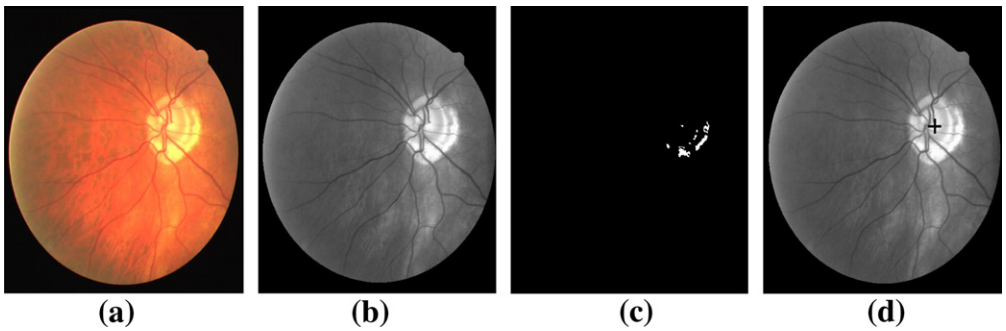

Fig. 2. (a) A image with non-uniform illumination (b) after illumination correction (c) candidate pixels (d) the estimated optic disc center (at black cross).

Using the contrast measure $(\mu_o - \mu_b)/(\mu_o + \mu_b)$, the contrast in the image is maximal when $N = 35$, where μ_o and μ_b represent the mean intensity value of optic disc pixels and that of background pixels, respectively.

2.1.2. Estimating optic disc center

In order to smooth noise and small area of bright lesions, an averaging filter of size 5×5 is applied to the illumination corrected image. The averaged image is then normalized to [0–255] intensity interval, and the highest 5% intensity pixels are selected as potential optic disc centers (Fig. 2(c)). For each candidate pixel, the local variation is calculated among adjacent pixels through a window size approximately equal to the optic disc dimensions. In this paper, the optic disc diameter is set to 90 pixels (one-sixth the width of the image). Since the property of the optic disc is characterized by high grey level variation, the candidate pixel having the highest variance value is considered the optic disc center (Fig. 2(d)). The subsequent processing can therefore work on the subimage that contains the optic disc region.

2.2. Optic disc boundary segmentation

The segmentation phase contains the Canny edge detector, the Hough transform, and the SGVF snake which consists of GVF snake deformation and contour supervised classification stage. Both of Canny edge detector and Hough transform are used to obtain the edge map, which is served as the initial contour in the snake deformation processing. Conventional GVF snake is not sufficient to segment contour due to vessel occlusion and fuzzy disc boundaries. In view of this reason, the SGVF snake is extended in each time of deformation iteration, so that the contour points can be classified and updated according to their corresponding feature information.

2.2.1. Extract initial contour

Considering that the optic disc shape is close to a circle or an ellipse, the initial boundary of the SGVF snake model is identified by applying the circular Hough transform to the edge map of the optic disc image. The purpose of the Hough transform is to find circular objects by transforming the edge map into a parameter space. The

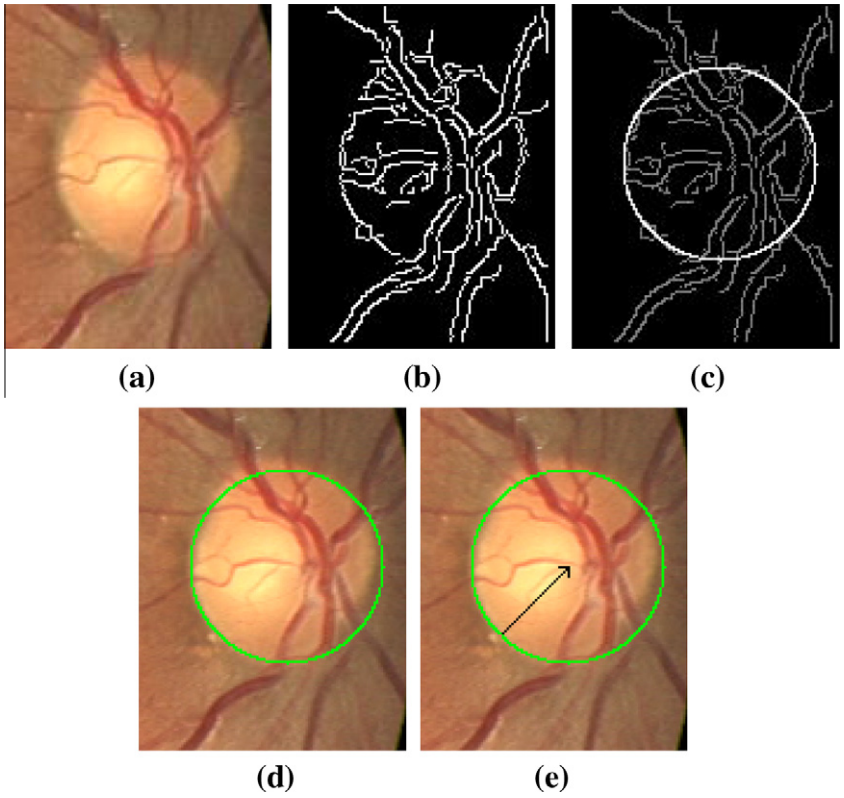

Fig. 3. Initial contour detection (a) optic disc image. (b) Edge map extracted from Canny edge detector. (c) The circular Hough transform (the bright circle overlaps the edge map). (d) Initial contour overlaps the optic disc image. (e) An example of feature vector extraction (the dark line).

edge map of the optic disc image is first extracted by means of Canny edge detector, and each edge point contributes votes to the parameter form for a circle $(x-a)^2+(y-b)^2=r^2$, where the (a,b) is the center of the circle of radius r that pass through edge point (x,y). Then, the maximum total vote of the parameter set (a,b,r) corresponds to the presence of the desired circle in the disc image. As shown in Fig. 3(c), the circular Hough transform is highly unaffected by image noise and broken boundaries due to the in-homogeneity inside the disc region.

2.2.2. Snake deformation

Snakes or active contour models (Kass, Witkin, & Terzopoulos, 1987) are deformable contour algorithms that minimize energy function in order to detect edges in a given image. The internal forces serve to ensure the spline has smoothness constraint, while the external force is responsible for pushing the snake toward subjective contours. The energy function of the snake is written as

$$E_{snake}=\int_0^1 E_{\text{int}}(c(s))+E_{ext}(c(s))ds = \int_0^1 \frac{1}{2}(\alpha|c'(s)|^2+\beta|c''(s)|^2)+E_{ext}(c(s))ds \quad (2)$$

where $c(s)=(x(s),y(s))$, $s\in[0,1]$, is a curve, and α and β are weighting parameters that control the snake's tension and rigidity, respectively.

It has been shown that finding the curve $c(s)$ which minimizes (2) is equivalent to solving the following equation

$$\alpha c''(s)-\beta c''''(s)-\nabla E_{ext}=0. \quad (3)$$

Consider the partial derivative of c with respect to time t and set

$$c_t(s,t)=\alpha c''(s,t)-\beta c''''(s,t)-\nabla E_{ext}. \quad (4)$$

Then when the solution $c(s,t)$ stabilizes, one achieves a solution of (3).

Traditional snakes model have difficulties associated with initial contours and the convergence of concave boundary regions. In general, snakes cannot move toward desired boundaries that are too far away, it cannot converge into concave objects, either. Hence, a external force for active contour called gradient vector flow (GVF) (Xu & Prince, 1998) is proposed. The GVF filed is defined as $\mathbf{v}(x,y)=[u(x,y),v(x,y)]$ that minimizes the energy function

$$\varepsilon=\iint \mu(u_x^2+u_y^2+v_x^2+v_y^2)+|\nabla f|^2|\mathbf{v}-\nabla f|^2dxdy \quad (5)$$

where $|\nabla f|$ is the gradient of the edge map and μ is a regularization parameter that can be set according to the proportion of noise in the image.

According to the consequences mentioned in Xu and Prince (1998), if value $|\nabla f|$ is small, the energy is dominated by the summation of the squares of the partial derivatives of the vector field u_x^2, u_y^2, v_x^2, v_y^2. On the other hand, if value $|\nabla f|$ is large, set $\mathbf{v}=\nabla f$ for minimizing the energy, e.g., $\mathbf{v}$ nearly equals the gradient of the edge map. The GVF can be obtained from the solution of the following Euler equations:

$$\mu\nabla^2 u-(u-f_x)(f_x^2+f_y^2)=0 \quad (6)$$

$$\mu\nabla^2 v-(v-f_y)(f_x^2+f_y^2)=0 \quad (7)$$

where ∇^2 is the Laplacian operator. The above equations can be solved by the numerical techniques.

Once the final GVF field $\mathbf{v}(x,y)$ is obtained, the following dynamic GVF snake equation

$$c_t(s,t)=\alpha c''(s,t)-\beta c''''(s,t)+\mathbf{v} \quad (8)$$

is applied to find the curve $c(s)$, which is the desired final contour. For more details, one is referred to (Xu & Prince, 1998). Also, an improved GVF snake method is provided by Liu et al. (2012).

2.2.3. Contour supervised classification

The GVF snake is not sufficient to locate the contour on the correct edge position in optic disc images due to the fuzzy edges and vessel occlusion. Since the external force of GVF snake derived from the edge map of the disc image, the blood vessels generate strong edges crossing the optic disc. Hence, the deformable model may converge to the false edge position. To overcome this problem, the contour points should be classified in each deformable process to identify the incorrect convergent points. The incorrect points will then adjust positions by using the information of the correct points. This iterative-update process is embedded into each snake deform iteration for reliable edge detection. The choice of an appropriate classifier has two considerations. First, the classifier should be robust against outliers form pathological changes in the training set. Second, the distribution of the feature vectors is unknown. To meet the requirements mentioned above, the Bayesian classifier has been chosen for determining whether the contour point is a correct point or not.

Base on the *a priori* knowledge that approximately 20% contour points are the vessel points (Xu et al., 2007), the contour points are classified into two classes, i.e., edge-point class and non-edge-point class. The prior probabilities are set to $P(ed)=0.8$ and $P(\neg ed)=0.2$ for the state of edge points and non-edge points, respectively. We use the intensity information of each contour point of the optic disc image to generate the feature vector $\mathbf{x}$ used in determining the conditional densities, $p(\mathbf{x}|ed)$ and $p(\mathbf{x}|\neg ed)$. The features are the intensity distribution of each contour point along radial line to the contour center as shown in Fig. 3(e), the contour center will be updated after each deformation. Each feature vector consists of two feature values denoted as: $\mathbf{x}_i=[mean(i),std(i)]^T$, where $mean(i)$ and $std(i)$ represent the mean and standard deviation of the intensity distribution of the

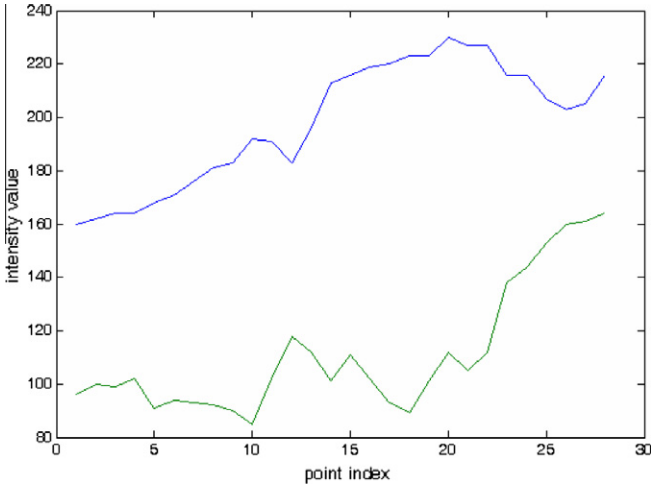

Fig. 4. The intensity distribution of a edge point (blue line) and a vessel point (green line). (For interpretation of the references to colour in this figure legend, the reader is referred to the web version of this article.)

Table 1
The success rates of optic disc localization methods.

Localization methods	DRIVE database (%)	STARE database (%)
Sinthanayothin et al. (1999)	60	50
Walter et al. (2002)	80	75
Proposed method	100	90

Table 2
Comparison of error distance and successful boundary.

Methods	Average error distance (pixels)	Standard deviation of error distance (pixels)	Successful boundary (%)
Proposed method (STARE database)	2.7	0.63	89
Proposed method (DRIVE database)	1.9	0.51	93
GVF snake (STARE database)	4.5	0.65	56
GVF snake (DRIVE database)	3.4	0.49	69

*i*th contour point. The intensity distribution will have different statistic depending on whether the contour point is located on the edge point or on the blood vessel point. If the contour point is located on the blood vessel point, the corresponding feature value should have lower intensity due to dark blood vessels (Fig. 4).

A multivariate normal density function is used to model the conditional densities (Duda, Hart, & Stork, 2001), which are defined as

$$p(\mathbf{x}|ed) = \frac{p_{ed}}{2\pi|\Sigma_{ed}|^{1/2}} e^{-(\mathbf{x}-\boldsymbol{\mu}_{ed})^t \Sigma_{ed}^{-1}(\mathbf{x}-\boldsymbol{\mu}_{ed})} \quad (9)$$

and

$$p(\mathbf{x}|\neg ed) = \frac{p_{\neg ed}}{2\pi|\Sigma_{\neg ed}|^{1/2}} e^{-(\mathbf{x}-\boldsymbol{\mu}_{\neg ed})^t \Sigma_{\neg ed}^{-1}(\mathbf{x}-\boldsymbol{\mu}_{\neg ed})} \quad (10)$$

where Σ_{ed} and $\sum_{\neg ed}$ are the covariance matrices and $\boldsymbol{\mu}_{ed}$ and $\mu_{\neg ed}$ are the population mean vectors generated from the training dataset for each class. The p_{ed} is a constant standing for the fractional contour of the optic disc while $p_{ed} = 1 - p_{\neg ed}$. In order to predict the class label of each contour point, $p(\mathbf{x}|C_i)p(C_i)$ for $i = 1, 2$ is calculated for each class C_i. The classifier predicts the class label of a contour point to be the class C_i if $p(\mathbf{x}|C_i)p(C_i)$ is the maximum.

The two class points are obtained after contour deformation and supervised classification. The points belonging to non-edge-point class will be updated to the correct positions by using the information of the edge-point class. Since the contour may converge toward the strong edges created by blood vessels during the deformable process, the concave boundaries are located at non-edge-points. As a result, the radius of each non-edge-point is replaced by the mean value of its first and second nearest neighboring edge points' radiuses along both sides. The resulted new contour is then used in the next snake deformation iteration. The algorithm will stop

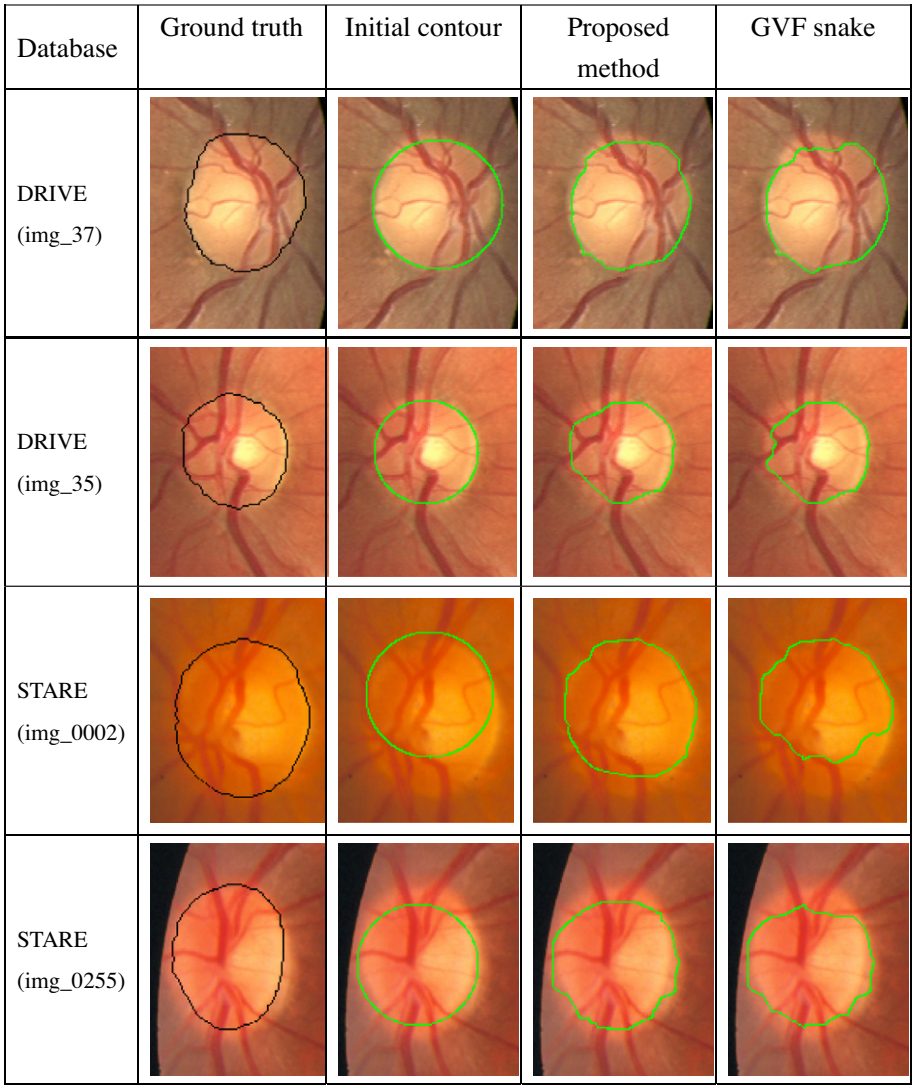

Fig. 5. Comparison of proposed method and GVF snake based on the same initial contour.

when the distance between the old contour and new contour is less than 1 pixel for five consecutive iterations.

3. Experimental results

To characterize the proposed algorithm for optic disc localization and segmentation over a large number of images, a comprehensive analysis on publicly available databases, Digital Retinal Images for Vessel Extraction (DRIVE) database (Research Section, 2009; Niemeijer, Staal, Van Ginneken, Loog, & Abramoff, 2004) and Structured Analysis of the Retina (STARE) database (Analysis of the Retina (STARE), 2009; Hoover, Kouznetsova, & Goldbaum, 2000), of color retinal fundus images is performed. The DRIVE database contains 40 images, with 565×584 pixels and 8 bits per color channel. These images were captured from a Canon CR5 nonmydriatic 3 charge-coupled device at 45° field of view, and compressed in JPEG format. The images are equally divided into a training set and a testing set, and the testing set has four images with pathology. The STARE database consists of 81 images captured by a TopCon TRV-50 fundus camera at 35° field of view. The images were digitized to 700×605 pixels, 8 bits per color channel. A subset of the STARE database is randomly selected to evaluate the performance of the proposed method.

In order to obtain a performance metric for this study, the correct localization criteria of the optic disc is defined based on a comparison of the estimated optic disc center to the manually selected center. The optic disc localization is considered to be correct if the distance between the estimated optic disc center and the manually selected center is less than one optic disc radius. The proposed optic disc localization method achieves a success rate of 90% in the subset of STARE database (i.e., the optic disc is correctly identified in 18 out of the 20 images). The average distance between the estimated optic disc center and the manually selected center is 23 pixels. In addition, the optic disc is successfully identified in all of the 40 DRIVE database images while using the proposed method. The average distance between the estimated optic disc center and the manually selected center is 15 pixels. The success rate compared with other localization methods are shown in Table 1.

In this study, a half of images in these two groups are used to train the Bayesian classifier. To produce the aggregate performance across the two databases, the testing data in the first group were exchanged to train the classifier and the original training data were taken as the testing images. The performance of the proposed optic disc segmentation method is also evaluated. The average error distance between the resulted boundary and the ground truth is calculated for evaluation. For each resulted contour point, the distance to the closest point of ground truth is used for calculation. Table 2 presents the maximum average error distance and standard deviation calculated with the proposed method and GVF snake for the testing images of each database, and the successful boundary indicates the true positive rate of the resulted boundary. The GVF snake parameters α and β are set to 1.0 and 0.1, respectively.

Fig. 5 shows the optic disc segmentation results compared with GVF snake method based on the same initial contour generated from the circular Hough transformation. Experiment results presents that the proposed method outperforms the conventional GVF snake method.

4. Conclusions

This paper proposes a method of automatic identification of the optic disc in retinal images, based on the illumination-correction operator and the SGVF snake algorithm. The proposed illumination correction operator generates significant contrast between the optic disc and background, which directly solves the problem of non-uniform illumination through the image. Our method takes advantage of the optic disc in the retina to extract the features of intensity distribution. These features are used to train the Bayesian classifier to classify the disc boundary into the correct contour point cluster or the vessel interference contour point cluster. The contour points are then updated into the correct disc edge locations after each GVF snake deformation. The overall performance is with 95% correct optic disc localization from the two publicly available databases used to evaluate the proposed illumination correction operator performance. The experimental result also shows that 91% disc boundaries are correctly segmented by the SGVF snake algorithm out of 60 images.

Acknowledgment

The authors thank A. Hoover for making his database publicly available.

References

Akita, K., & Kuga, H. (1982). A computer method of understanding ocular fundus images. *Pattern Recognition, 15*, 431–443.

Aquino, A., Gegúndez-Arias, M. E., & Marín, D. (2010). Detecting the optic disc boundary in digital fundus images using morphological, edge detection, and feature extraction techniques. *IEEE Transactions on Medical Imaging, 29*, 1860–1869.

Duda, R. O., Hart, P. E., & Stork, D. G. (2001). *Pattern classification*. New York: Wiley.

Foracchia, M., Grisan, E., & Ruggeri, A. (2004). Detection of optic disc in retinal images by means of a geometrical model of vessel structure. *IEEE Transactions on Medical Imaging, 23*, 1189–1195.

Hoover, A., & Goldbaum, M. (2003). Locating the optic nerve in a retinal image using the fuzzy convergence of the blood vessels. *IEEE Transactions on Medical Imaging, 22*, 951–958.

Hoover, A., Kouznetsova, V., & Goldbaum, M. (2000). Locating blood vessels in retinal images by piecewise threshold probing of a matched filter response. *IEEE Transactions on Medical Imaging, 19*, 203–210.

Kass, M., Witkin, A., & Terzopoulos, D. (1987). Snake: Active contour model. *International Journal of Computer Vision, 1*, 321–331.

Lalonde, M., Beaulieu, M., & Gagnon, L. (2001). Fast and robust optic disc detection using pyramidal decomposition and Hausdorff-based template matching. *IEEE Transactions on Medical Imaging, 20*, 1193–1200.

Lalonde, M., Gagnon, L., Boucher, M. C. (2000). Non-recursive paired tracking for vessel extraction from retinal images. In *Proc. of the conf. vis. interface, Montreal, Canada* (pp. 61–68).

Li, H., & Chutatape, O. (2004). Automated feature extraction in color retinal images by a model based approach. *IEEE Transactions on Biomedical Engineering, 51*, 246–254.

Liu, C. C., Tsai, C. Y., Tsui, T. S., & Yu, S. S. (2012). An improved GVF snake based breast region extrapolation scheme for digital mammograms. *Expert Systems with Applications, 39*, 4505–4510.

Lowell, J., Hunter, A., Steel, D., Basu, A., Ryder, R., Fletcher, E., et al. (2004). Optic nerve head segmentation. *IEEE Transactions on Medical Imaging, 23*, 256–264.

Lu, S., & Lim, J. H. (2011). Automatic optic disc detection from retinal images by a line operator. *IEEE Transactions on Biomedical Engineering, 58*, 88–94.

Manivannan, A., Sharp, P. F., Phillips, R. P., & Forrester, J. V. (1993). Digital fundus imaging using a scanning laser ophthalmoscope. *Physiological Measurement, 14*, 43–56.

Niemeijer, M., Staal, J., Van Ginneken, B., Loog, M., Abramoff, M. D. (2004) Comparative study of retinal vessel segmentation methods on a new publicly available database. In Fitzpatrick, J. M., Sonka, M. (Eds.), *SPIE Med. Imag.* (Vol. 5370, pp. 648–656).

Osareh, A. (2004). Automated identification of diabetic retinal exudates and the optic disc. Dissertation, University of Bristol.

Research Section, Digital Retinal Image for Vessel Extraction (DRIVE) Database. (2009). Utrecht, The Netherlands, Univ. Med. Center Utrecht, Image Sci. Inst. <http://www.isi.uu.nl/Research/Databases/DRIVE>.

Sinthanayothin, C., Boyce, J. F., Cook, H. L., & Williamson, T. H. (1999). Automated localization of the optic disc, fovea, and retinal blood vessels from digital color fundus images. *British Journal of Ophthalmology, 83*, 902–910.

Structured Analysis of the Retina (STARE) Project Website. (2009). Clemson, SC, Clemson Univ. <http://www.clemson.edu/ces/>.

Taylor, H. R., & Keeffe, J. E. (2001). World blindness: A 21st century perspective. *British Journal of Ophthalmology, 85*, 261–266.

Ter Haar, F. (2005). Automatic localization of the optic disc in digital colour images of the human retina. Dissertation, University of Utrecht.

Tobin, K. W., Chaum, E., Govindasamy, V. P., & Karnowski, T. P. (2007). Detection of anatomic structures in human retinal imagery. *IEEE Transactions on Medical Imaging, 26*, 1729–1739.

Tolias, Y. A., & Panas, S. M. (1998). A fuzzy vessel tracking algorithm for retinal images based on fuzzy clustering. *IEEE Transactions on Medical Imaging, 17*, 263–273.

Walter, T., Klein, J. C., Massin, P., & Erginary, A. (2002). A contribution of image processing to the diagnosis of diabetic retinopathy-detection of exudates in color fundus images of human retina. *IEEE Transactions on Medical Imaging, 21*, 1236–1243.

Xu, J., Chutatape, O., Sung, E., Zheng, C., & Kuan, P. (2007). Optic disk feature extraction via modified deformable model technique for glaucoma analysis. *Pattern Recognition, 40*, 2063–2076.

Xu, C., & Prince, J. L. (1998). Snakes, shapes, and gradient vector flow. *IEEE Transactions on Image Processing, 7*, 359–369.

Youssif, A. A. A., Ghalwash, A. Z., & Ghoneim, A. S. (2007). A comparative evaluation of preprocessing methods for automatic detection of retinal anatomy. In *Proc. 5th Int. Conf. Inform. Syst.* (pp. 24–30).